

School of Electronics and Computer Science
Faculty of Engineering, Science and Mathematics
UNIVERSITY OF SOUTHAMPTON

Alex Beharrell

May 3, 2011

**Converting an Inexpensive RC
Helicopter into an Autonomous Vehicle**

Project supervisor: Dr Reuben Wilcock
Second examiner: Dr Tom J Kazmierski

A project report submitted for the award of
MEng Electronic Engineering

ABSTRACT

In the modern world there are many situations that could benefit from the use of autonomous aerial vehicle platforms, mainly those that involve remote sensing, however, traditional UAVs (unmanned aerial vehicles) are often prohibitively expensive. Recently there has been an increase in inexpensive remote control helicopters due to advances in technology allowing the simplification of control systems by mechanical stabilisation. This project used this increased availability and simplicity in order to construct an autonomous aerial vehicle platform, making use of the mechanical stabilisation to save cost and complexity in the control systems of the helicopter.

An autopilot was produced to control a consumer remote control helicopter, with software allowing it to stabilise itself in the pitch and yaw axes. The autopilot could also make basic observations of its environment. The autopilot could not completely determine its linear position and so the degree of autonomy possible was limited.

The project showed the possibility of using similar techniques to extend the functionality and so construct a more autonomous vehicle with greater potential use for remote sensing applications while remaining less expensive than traditional aerial vehicle platforms.

Acknowledgements

I would like to thank my supervisor, Dr Reuben Wilcock, for advice and support given throughout the project.

Statement of Originality

All code for the autopilot and the ground station user interface has been written by me, with the exception of various software libraries referenced below. The designing of the system has been my own work and any designs that have been adapted have been referenced in the main body of the report.

The autopilot software used 'avr-libc' [1] to provide standard C language features and Peter Fleury's I²C library [14] for communications with the sensors.

The ground station software used the QT framework [2] to speed up development of the user interface. Communication with a joystick and by serial port were provided by 'libjoystick++' [18] and Terraneo Federico's QAsyncSerial class [13], respectively. The QAsyncSerial class used the Boost C++ libraries [3] for low-level interfacing with the serial port.

Contents

Acknowledgements	ii
Statement of Originality	ii
1 Introduction	1
1.1 Project Scope	1
2 Literature Review	3
2.1 Helicopter Operation	3
2.1.1 Stabiliser Bar	4
2.1.2 Motor Control	4
2.2 Sensor Data Reading and Processing	4
3 Design Choices	6
3.1 Helicopter	6
3.2 Microcontroller	7
3.2.1 Choice of Microcontroller	7
3.2.2 Program Design	7
3.3 Circuit Board	8
3.3.1 Type of Board	8
4 System Implementation	10
4.1 Initial Microcontroller Experimentation	10
4.2 State Machine	10
4.3 Communications	11
4.3.1 Wired Communications	11
4.3.2 Wireless Communications	11
4.4 User Interface	13
4.5 Transistor Circuits and Motor Control	14
4.6 Sensor Data	15
4.7 PCB Design and Manufacture	18
4.7.1 Power Supply Decoupling	19
4.8 PID Controller	20
4.9 Environment Mapping	23
5 System Testing and Results	24

5.1	Power Supply	24
5.2	Remote Control	27
5.3	PID Tuning	28
5.3.1	Pitch Control	28
5.3.2	Heading Control	30
5.4	Environment Mapping	30
6	Evaluation	32
6.1	Fulfilment of Scope	32
6.2	Project Management	33
6.3	Further Work	33
7	Conclusion	36
A	Original Project Brief	38
A.1	Problem	38
A.2	Goals and Scope	38
B	Autopilot Registers	39
C	Communications Protocol	40
D	Communications Protocol Commands	41
E	Circuit Schematic	42
F	Helicopter Diagram	45
G	Code Listings	46
H	Costing	49
I	CD Table of Contents	50
	Bibliography	52

List of Figures

2.1	Helicopter Flight Vectors (from [24])	3
2.2	Rotation representations	5
4.1	State Machine - Main Program	11
4.2	State Machine - UART Reading	12
4.3	Serial communications user interface	13
4.4	Serial communications user interface - second version	14
4.5	Calculations to control motors from heading data	15
4.6	State Machine - Timed Commands / Reading of Sensors	16
4.7	Calibration of magnetometer	17
4.8	Calculations to normalise magnetometer readings	18
4.9	Flow of data through autopilot	21
4.10	Orientation of sensor stick with respect to helicopter (from [28]) . .	22
5.1	Positive supply rail measured at motor	25
5.2	Positive supply rail measured at digital supply (with additional de- coupling)	25
5.3	MOSFET gate RC time constant	26
5.4	MOSFET gate rise time	26
5.5	Effect of framing on RF receiver synchronisation	27
5.6	Pitch PID tuning setup	29
5.7	Environment Mapping - Initial Test	31
6.1	Gantt Charts	35
E.1	Circuit Schematic - AVR	42
E.2	Circuit Schematic - Power Distribution	43
E.3	Circuit Schematic - Motors	43
E.4	Circuit Schematic - PCB	44
F.1	Helicopter Diagram	45
F.2	Helicopter Photograph	45

List of Tables

3.1	Comparison of different types of helicopter	6
3.2	Comparison of different types of circuit board	8
4.1	Different areas of circuitry for autopilot	19
B.1	Status and Control Registers	39
C.1	Communications Protocol Format	40
D.1	Commands in the communications protocol	41
H.1	Costing of autopilot prototype	49

Listings

G.1	Macros used to access status and control registers	46
G.2	PID data structure	46
G.3	PID processing function	46
G.4	Magnetometer calibration	47
G.5	Calculated mode of motor control	47

1. Introduction

Unmanned aerial vehicles (UAVs) offer significant advantages for remote sensing applications, particularly those concerned with dangerous or difficult to navigate situations. However, the cost of traditional UAVs often prohibits their use and so it would be desirable for an inexpensive aerial sensing platform to be available. The use of an air based solution over a ground based one offers the advantage of being able to navigate difficult terrain far more easily which can reduce the cost by reducing the complexity of the solution. The use of balance bars (as explained in Section 2.1.1) to provide mechanical stabilisation has increased availability of inexpensive remote control helicopters and also provides a potential way to reduce the complexity of control systems needed for a rotary-wing UAV. The aim of the project is to adapt a mechanically stabilised consumer remote control helicopter to allow autonomous control by constructing an autopilot, providing an inexpensive platform for applications which require or could benefit from an autonomous aerial vehicle. Also, the project will help to show the viability of using mechanical stabilisation for other autonomous rotary-wing aerial vehicles.

The main basis for the autopilot will be a microcontroller which will be responsible for controlling the helicopter in a stable manner. The microcontroller would also be responsible for acquiring sensor data in order to be able to build up a picture of its environment and the orientation of the helicopter relative to its environment (the attitude of the helicopter). Communication with a ground station will also be needed to provide additional control of the autopilot and to retrieve data for later processing.

1.1 Project Scope

- Control of helicopter by microcontroller

The first step is to build a system which is able to control the motors of the chosen helicopter which can then be expanded upon to provide the rest of the functionality required by the autopilot.

- Communication between the helicopter and a ground station

A communication link will be needed to transfer data and commands between the microcontroller and the ground station. Wireless communications will be necessary for the autopilot as the ground station will need to be able to have some degree of control while the helicopter is flying.

- Attitude determination and stabilisation

The microcontroller would be responsible for the acquisition and processing of sensor data in order to calculate the attitude of the helicopter. The ability to sense the attitude, combined with control of the motors will allow control of the attitude and therefore stable flight. From stabilised flight the controller would be adapted to also allow controlled movement of the helicopter.

- Environment mapping

The autopilot will utilise proximity sensors which would be used for collision detection and avoidance. The autopilot will use the communications link to transmit the sensor data to the ground station which will combine the distance readings with the current position and attitude of the helicopter to build up a model of the environment.

2. Literature Review

Research for the project focused on two main areas, details of the helicopters operation so that the autopilot design could reflect the chosen helicopter and also on reading and processing of sensor data to be used to control the helicopter. The majority of mechanically stabilised remote control helicopters use a similar design that consists of two coaxial rotors that produce the lift used to keep the helicopter aloft with a tail rotor that controls the pitch of the helicopter. The reasons for choosing this type of helicopter and its advantages and disadvantages are discussed in Section 3.1.

2.1 Helicopter Operation

The helicopter used for the project [19] is a three channel helicopter which uses a coaxial design. The two rotors spin in opposing directions to cancel torque produced by the rotors and stop unwanted yawing [11]. Varying the relative speeds of the two rotors results in a yawing motion and control of the heading. Vertical motion is controlled by varying both rotors by the same amount so the lift varies while overall torque is kept the same. The pitch of the helicopter is controlled by using the tail rotor which produces a turning moment around the centre of gravity. The horizontal speed of the helicopter is controlled by changing the pitch and therefore creating a resultant force forwards or backwards as shown in Figure 2.1.

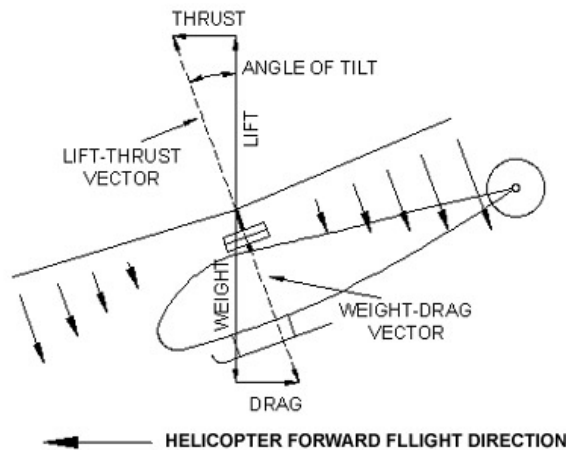


FIGURE 2.1: Helicopter Flight Vectors (from [24])

2.1.1 Stabiliser Bar

Roll control on the chosen helicopter is achieved with a stabiliser (or balance) bar which changes the cyclic pitch of the main rotor. This is a purely mechanical system and makes the helicopter resistant to changes in angle of bank. The stabiliser bar works similarly to the Bell-Hiller system used on some full sized helicopters [21]. However, rather than mixing the stabilising action with a control input the cyclic pitch is only controlled by the stabiliser. By placing a small weight at both ends of the stabiliser bar and connecting it to the motor shaft it acts as a gyroscope when the main rotor is spinning. A gyroscope resists any motion in the plane of rotation and when the helicopters angle of bank changes the stabiliser bar is at a different angle to the motor shaft resulting in a cyclic input correcting the unwanted roll [16].

2.1.2 Motor Control

The original controller on the chosen helicopter, used for manual remote controlled flight, used pulse width modulation to control the motors as it provides a way to control the amount of power delivered to the motors with a digital signal [32]. Varying width pulses are sent to the motor which results in an amount of power delivered to the motors proportional to the width of the pulse. Also, a switching circuit will need to be designed as a microcontroller will not be able to supply sufficient current to drive the motors.

2.2 Sensor Data Reading and Processing

Two sets of data are necessary to control the helicopter and retrieve data about the environment. The attitude of the helicopter is the representation of its rotational position compared to a reference frame and combined with the linear position provides sufficient information to determine the helicopters position in space.

The attitude of a body is defined as the difference between the bodies frame and the reference (fixed) frame which for the purpose of this project is taken as the earth [26]. There are different methods of representing the rotations that define the attitude with their own advantages and disadvantages. Euler angles correspond to the angles of rotation directly but are dependent on the order applied and contain singularities at the extremes of rotations. Both quaternions and direction cosine

matrices solve these problems. The representations and their relation to each other are shown in Figure 2.2.

$$\begin{array}{c}
 \text{given a rotation of axis } \rightarrow \mathbf{e} = \begin{bmatrix} e_x \\ e_y \\ e_z \end{bmatrix} \text{ and angle } = \theta \\
 \\
 \text{Quaternions } \rightarrow \mathbf{q} = \begin{bmatrix} q_1 \\ q_2 \\ q_3 \\ q_4 \end{bmatrix} \quad \begin{array}{l} q_1 = e_x \sin \frac{\theta}{2} \\ q_2 = e_y \sin \frac{\theta}{2} \\ q_3 = e_z \sin \frac{\theta}{2} \\ q_4 = \cos \frac{\theta}{2} \end{array} \\
 \\
 \text{Rotation matrix } \rightarrow \mathbf{R} = \begin{bmatrix} \cos \theta + e_x^2 (1 - \cos \theta) & e_x e_y (1 - \cos \theta) - e_z \sin \theta & e_x e_z (1 - \cos \theta) + e_y \sin \theta \\ e_y e_x (1 - \cos \theta) + e_z \sin \theta & \cos \theta + e_y^2 (1 - \cos \theta) & e_y e_z (1 - \cos \theta) - e_x \sin \theta \\ e_z e_x (1 - \cos \theta) - e_y \sin \theta & e_z e_y (1 - \cos \theta) + e_x \sin \theta & \cos \theta + e_z^2 (1 - \cos \theta) \end{bmatrix}
 \end{array}$$

FIGURE 2.2: Rotation representations

It is possible to build up rotation matrices directly from sensor data as shown in [26]. Once the attitude is represented in the form of a rotation matrix (or directional cosine matrix) it is possible to retrieve the roll, pitch and yaw angles by performing certain dot or cross products which only require multiplication and addition, significantly reducing the computation time when performed on a microcontroller. Quaternion or Euler angle representation would require trigonometric calculations resulting in a significant delay.

As the helicopter used has mechanically controlled roll only the pitch and yaw angles vary. Therefore the full rotational representation is not needed as the controller can act solely on these two angles. Although Euler angles have singularities at the extremes of rotation this does not matter significantly due to the lack of movement about the roll axis. The values of pitch should not vary by more than a few degrees as beyond small values of pitch the helicopter will become unstable. The singularities will be relevant for the heading (yaw angle) as when at a heading of 180° there is a sudden change from $+180^\circ$ to -180° . Due to the design of the helicopter each axis has little effect on the other axes and so this singularity can be dealt with by the controller as it only exists for one specific case.

3. Design Choices

The choice of components for the autopilot was, in part, influenced the the components used by the original controller of the helicopter, as they were known to work with the chosen helicopters motors and battery.

3.1 Helicopter

There are three main types of remote control helicopter available as shown in Table 3.1. The cost of a helicopter is usually closely related to the power of the rotors and so therefore the helicopters carrying capacity.

No. of Channels	Up/Down	Yaw	Pitch	Roll	Cost and Capacity
2	X	X			Low
3	X	X	X		Medium
4	X	X	X	X	High

TABLE 3.1: Comparison of different types of helicopter

Two channel helicopters were initially investigated as they are the lowest cost RC helicopters available, however they are mostly limited to a carrying capacity of a few grams. Even if a more substantial 2-channel helicopter could be found there is no control of pitch available as they instead rely on always travelling forward at a fixed speed which would require complex control in order to be used for a practical application.

As four channel helicopters do not have the mechanical stabilisation of roll found on three channel helicopters a complex controller is needed as both pitch and roll have to be stabilised electronically. Also, a movement in one axis will influence the other axes further increasing complexity. Despite the greater flexibility of a 4-channel helicopter and increased carrying capacity the greater complexity and cost mean that it would not entirely be in line with the project goals.

A three channel helicopter was chosen as it offers the best balance between flexibility and cost, it was decided that the inability to correct lateral movement could be overcome and was not sufficiently disadvantageous to justify increasing cost. There

are two common designs of three channel helicopters, coaxial helicopters which have two contra-rotating rotors on the same axis and tandem helicopters which have counter-rotating rotors mounted on different axes on the body of the helicopter. Helicopters of a coaxial design are more common and so it was easier to find one of a suitable cost and carrying capacity and hence a coaxial helicopter was used for this project.

3.2 Microcontroller

3.2.1 Choice of Microcontroller

There were three microcontrollers considered for being used for the autopilot, either an 8-bit AVR or PIC or an ARM based microcontroller.

Both 8-bit microcontrollers are comparable in terms of processing power and on-board peripherals and although the processing power is limited compared to an ARM based microcontroller, development is easier due to greater familiarity, specifically with AVR microcontrollers. It was decided that due to the existence of projects such as Ardupilot [4] which uses an AVR based controller, the added complexity of an ARM based microcontroller would not be needed.

The use of an AVR microcontroller was decided on as it offered more on-board peripherals than PIC microcontrollers, for example the PIC16F874 [22] has two PWM outputs while the ATmega8 [9] has three PWM outputs. The requirements of the project could therefore be met with a lower complexity AVR than a PIC. Also, it had the benefit of added familiarity with the architecture and development tools.

3.2.2 Program Design

As the autopilot is controlling the helicopter in flight it is particularly important that it can respond in a timely fashion to irregular events, whether they are commands from the ground station or changes in the sensor data which indicate the need for action to return to the desired attitude. For this reason the program running on the autopilot would be designed like a state machine as this would improve its ability to respond to incoming events of different types. Incoming events would result in interrupts being triggered on the microcontroller and so flags could be used to

signify the presence of events to the main state machine which would then be dealt with when the processing of other previous events had finished.

In order to stabilise the helicopter a closed loop controller would be needed and so a discrete proportional-integral-derivative (PID) controller would be used. The sampling rate of the sensor data would determine the sampling rate used for the PID algorithm. A PID controller was chosen due to familiarity with techniques for their design and testing as well as examples that demonstrated that such a controller could be implemented on an AVR, such as Atmel application note 'AVR221' [6].

3.3 Circuit Board

3.3.1 Type of Board

The construction of the circuit board used to mount the components on the helicopter was important as weight is an important factor due to limited carrying capacity. Also, ideally the board would be low cost to further reduce expense.

Two main options were available for use, stripboard and printed circuit boards. With printed circuit boards there was either the option of small scale, milled or etched (toner transfer method) boards, or a commercially produced circuit board.

Type	Design Time	Manufacture Time	Weight	Cost
<i>Stripboard</i>	Low	High	High	Low
<i>Milled PCB or Etched PCB</i>	High	Low	Low	Low
<i>Commercial PCB</i>	High	High	Low	High

TABLE 3.2: Comparison of different types of circuit board

Table 3.2 shows the advantages and disadvantages of the different types of boards. Weight and cost were the most important factors for the project and so neither stripboard or commercial PCBs were suitable. Stripboard is not particularly space efficient and would require the use of through hole components, significantly adding to the weight of the autopilot. A commercial PCB would increase the cost of the autopilot too much for prototyping but would be suitable as a way to implement a finished version as commercial PCBs are more suited to volume production than prototyping.

The decision was made to use an etched PCBs as it had some advantages over a milled PCB. The etched boards could have smaller traces as the process was limited by the resolution of a printer rather than the mechanical precision of a CNC machine. Theoretically traces down to around $\frac{2}{300}$ inch could be produced [31] but this was far smaller than needed for the autopilot. The toner transfer method did have the disadvantage of not always producing well defined traces, but any problems could be determined before any copper was removed.

4. System Implementation

4.1 Initial Microcontroller Experimentation

Initially the environment needed to program the AVR was set up, breadboard was used to allow rapid prototyping of different circuits which were then transferred to a PCB for the final design. During this stage it was verified that the AVR's three PWM outputs could be used independently to control all three motors. The AVR was programmed using C, compiled with `avr-gcc` as although less efficient than assembly it offered quicker development.

4.2 State Machine

Due to the reasons stated in Section 3.2.2 the program was designed in the style of a state machine. Sensor data and command input is interrupt based and the interrupt service routines (ISRs) were designed to store the data for processing in the main state machine. This required the use of a status register so different parts of the program could be notified of the presence and source of new data, a control register was also utilised so that different modes of operation could be supported. The contents and operation of the registers are explained in Appendix B.

The C preprocessor was used to simplify the use of the status and control registers. Each bit was defined and accessed by name so it was clear which bit was intended and this also allowed re-ordering of the registers without changing the rest of the program. Macros were written to allow each bit to be set, cleared and checked individually which also ensured that the registers were accessed in a consistent way (as shown in Listing G.1).

Figure 4.1 shows the design of the state machine. Each state in the state machine, and the ISRs, were designed to be run as quickly as possible so that the timing was as consistent as possible with data arriving asynchronously. The processing of data, which occurred in the `ST_INT_COMMAND` (internal command processing) state, was the most computationally complex component of the program as it involved floating point arithmetic which is not supported natively by the AVR microcontroller and hence required more clock cycles to perform the calculations.

The sample rate for the sensors had be calculated (as shown in Section 4.6) to ensure that there were still sufficient processor cycles available to process commands before more sensor data needed to be calculated.

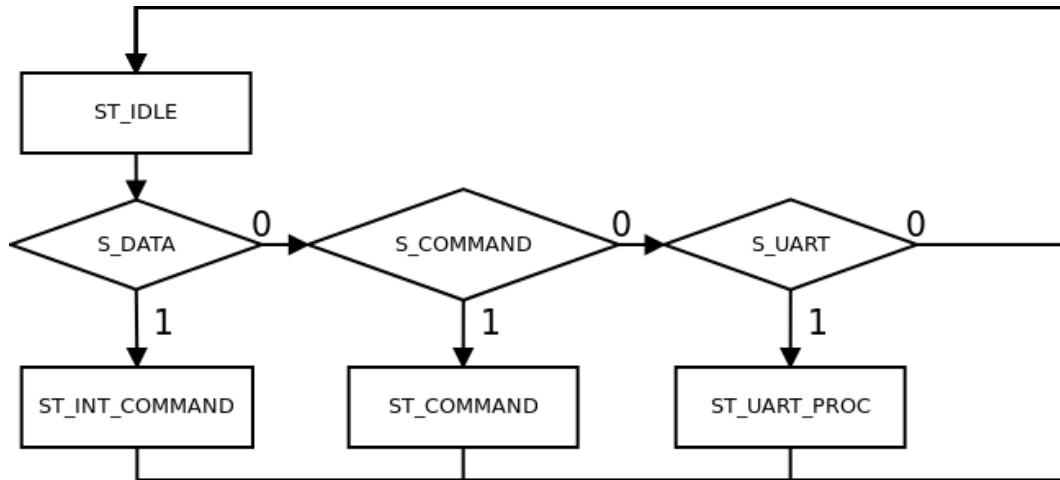


FIGURE 4.1: State Machine - Main Program

4.3 Communications

4.3.1 Wired Communications

A wired link was initially used for debugging and control of the microcontroller. The link was between the UART (universal asynchronous receiver/transmitter) on the AVR and a USB-to-Serial converter on the ground station (a laptop running Linux). The use of a communications protocol allowed the link to more easily transfer different types of data. The protocol is explained further in Appendix C and the commands are described in Appendix D.

4.3.2 Wireless Communications

The same communications protocol was used for the wireless link between the ground station and the autopilot but a simple ASK transmitter/receiver pair was used which only allowed one-way communication from the ground station to the autopilot. The ground station only needed to receive information for further processing which could take place over a wired connection at the end of each flight. The limitations of a one-way link were justified by reducing the complexity of the

autopilot. This also meant that many of the commands, those responding to the ground station, were no longer needed.

The receiver on the autopilot was limited to a data rate of about 2400 bps [29] which was significantly slower than the previous wired link. Also, the receiver requires frequent transitions between '0' and '1' to synchronise itself with the transmitter. In order to provide this synchronisation framing was added around each byte of a sent command and the ground station would continuously transmit alternating 1's and 0's ('U' in ASCII) while there were no commands to send. A state machine (Figure 4.2) was added to the UART ISR to process this framing and place the received command into a buffer.

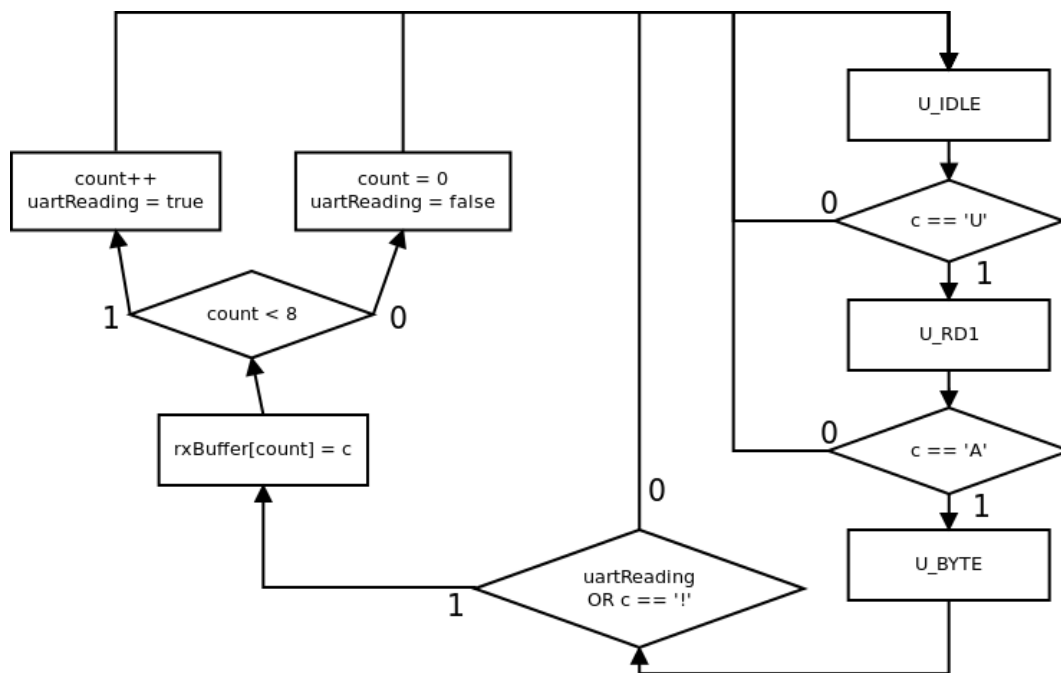


FIGURE 4.2: State Machine - UART Reading

The framing ensured a minimum number of transitions per byte of each command. As before, the state machine would stay idle until it detected a start character however the length of commands was fixed to 8 bytes for the wireless communications link as, due to the inherent unreliability, it was possible for a character to be lost and if the byte signifying the end of the command was lost it could cause further problems as the state machine would continue to try to read in the command until the next stop byte was received.

4.4 User Interface

A graphical user interface was written to control communications between the ground station and the helicopter. The code for the user interface was, in part, generated using QT Designer [2]. The code for the backend of the user interface was written in C++ using the QT UI library, allowing the reuse of C code, such as the defaults for the control register. The initial design of the interface is shown in Figure 4.3 and was designed for two way communication between the autopilot and ground station. When the communications link changed to being a one-way wireless connection the user interface was redesigned to better suit the new requirements. Both versions of the user interface allowed commands to be easily sent to the autopilot by taking care of the communications protocol.

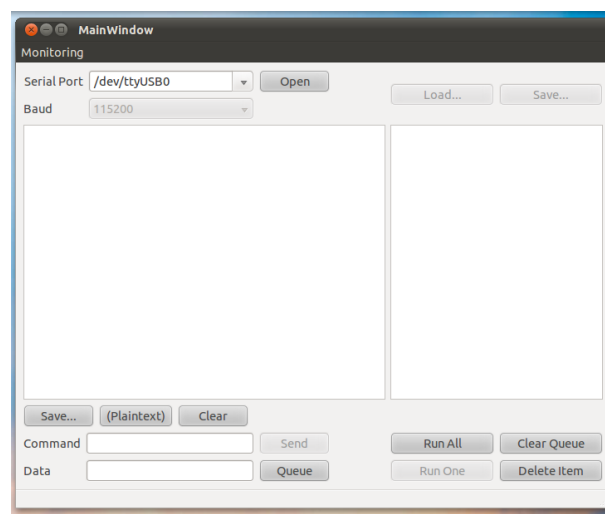


FIGURE 4.3: Serial communications user interface

The second version of the user interface, as shown in Figure 4.4, was primarily used to send commands as there was only one-way communication from the ground station to the autopilot. The second version of the user interface gave easier access to common commands and features of the autopilot. The state of the control register is shown in the interface and toggling any of the bits will send the relevant command, also a section was added to allow the magnetometer to be more easily calibrated. Buttons were also added both for common commands and also to set the relevant command byte characters, for example 'Prepare 2' would put 'p' into both 'c1' and 'c2' to set pitch PID constants (Appendix D).

For later testing of the autopilot it was planned to control the helicopter manually and then test PID control of each of the axes separately. This would allow individual tuning of each PID controller which would simplify testing. In order to allow manual

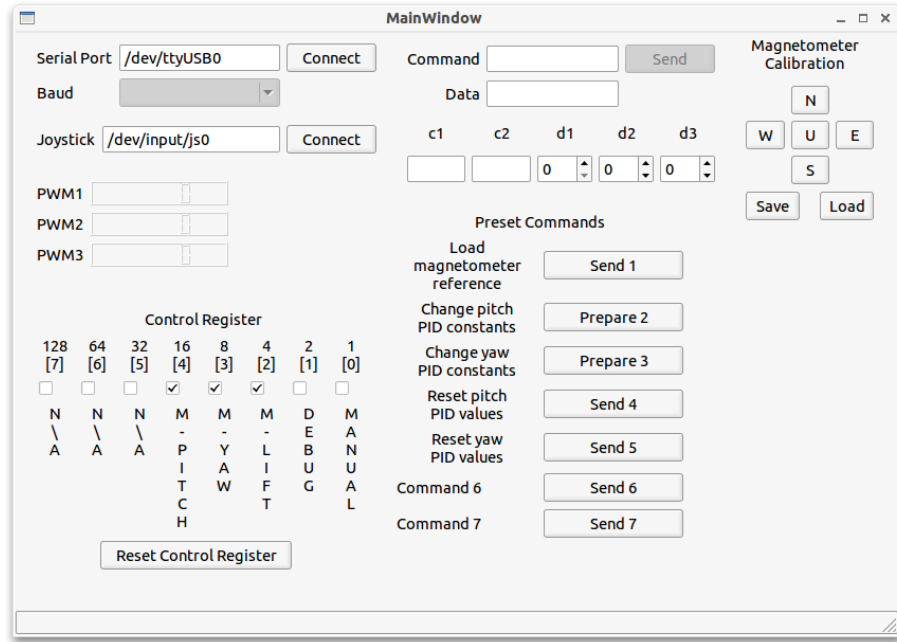


FIGURE 4.4: Serial communications user interface - second version

control of the helicopter input from a joystick to the ground station was needed as keyboard control would not offer sufficiently precise control to be able to fly the helicopter. To achieve joystick control values were read from a Playstation 3 'Sixaxis' controller. The values of the joystick were read every 115 ms (to allow sufficient time for the necessary commands to be sent to the autopilot) and sent to the helicopter as values of lift, yaw and pitch.

4.5 Transistor Circuits and Motor Control

The maximum current supplied by any individual pin on the AVR is 40 mA [8] and the helicopter was found to need ≈ 1 A for the main rotors and ≈ 0.2 A for the tail rotor. To deliver the needed current a NMOS transistor was used to switch the power to the motor, with the gate connected to the PWM outputs of the AVR so that motor current depended on the PWM duty cycle. Transistors with low R_{on} had to be chosen as the equivalent resistance of the motors was very low and a voltage divider existed with the motor and transistor, giving a voltage across the motor of $V_{motor} = \frac{R_{motor}}{R_{motor} + R_{on}} V_{dd}$ and so R_{on} needed to be minimised to minimise power lost to the MOSFET. The tail rotor required an H-Bridge to change the direction of the motor and effect positive and negative changes in pitch. The design of the H-Bridge was adapted from [10] and pull-up resistors were added to the direction signals to ensure that the H-Bridge would be in a known state even if the gates

were un-driven. A PWM frequency of 3.125 kHz was chosen as it was close to the frequency used by the original controller (2.27 kHz).

To ensure that the chosen transistors would be able to switch sufficient current to control the motors transistors with similar characteristics to the transistors used on the helicopters original control board were chosen. Particular attention was given to the ratings for maximum current and R_{on} values. The final schematic of the motor control circuitry is shown in Figure E.3. Also, although the rating of the MOSFET's body diode was sufficient to protect the transistor from spikes caused when the motor is switched off, the circuit requires a further protection diode to carry the excess charge to ground and prevent excessive changes to the supply voltage.

The AVR could control the speed of the three motors by changing the PWM duty cycles, and could control the direction of the tail rotor by two outputs (DIR1 and DIR2) which were connected to the H-Bridge. Initially the motors were controlled directly but due to the coaxial design of the helicopter it was desirable to have two modes of operation, directly driving the motors and 'calculated' control where values for lift, yaw and pitch were used to calculate the needed motor inputs as shown in Figure 4.5. The C implementation of the calculated mode is shown in Listing G.5. The calculated control takes inputs from both the ground station and the PID controller and these different modes are selected by the control register as shown in Table B.1.

$$\begin{aligned} Motor_{Main} &= Lift + Yaw \\ Motor_{Secondary} &= Lift - Yaw \\ Motor_{Tail} &= |Pitch| \end{aligned}$$

(Where all three values are restricted to a range of $0 \rightarrow 255$)

$$DIR1 = Pitch > 0, DIR2 = Pitch < 0$$

FIGURE 4.5: Calculations to control motors from heading data

4.6 Sensor Data

Initially the autopilot used the Dimension Engineering DE-ACCM3D (which contained an ADXL330 accelerometer), allowing the tilt of the helicopter to be determined for both the roll and pitch axes. This allowed control of the pitch axis but additional sensors were needed to control the heading. A three axis gyroscope would give measurements for the rate of change of heading, as well as pitch, but

due to numerical errors [26] a reference for the heading was also needed which could be provided by a three axis magnetometer. Using three separate sensors would add weight to the autopilot and so for the final design the Sparkfun SEN-10321 'Sensor Stick' was used which provided an accelerometer (ADXL345), a gyroscope (ITG-3200) and a magnetometer (HMC5843) all of which were three axis sensors.

The AVR was used to communicate with the I²C interface to the sensor stick. Peter Fleury's I²C library [14] was used to control and read the sensors and wrapper functions were written to simplify the reading of each sensor as they all had similar requirements for reading. All three sensors output 16-bit signed integers (in two's complement format) which could be directly used for calculations in C but required extra cycles to compute as the AVR is only an 8-bit processor.

The sample rates varied between the sensors but the magnetometer had the lowest sample rate at a maximum of 50Hz [17]. One of the AVR's timers was set up to allow the sensors to be read at a fixed time interval by causing an interrupt to be signalled regularly. In order to make sure the sensors were read at a fixed interval the communications between the AVR and the sensors took place within the ISR. At an I²C clock of 100 kHz it takes 810 μ s to read all three values from one sensor (including protocol overhead there are 81 bits communicated) so to read all three sensors would take 2.43 ms. As the UART operates at 2400 bps each byte takes 3.3 ms to transmit, meaning the UART ISR is triggered every 3.3 ms. If interrupts are disabled, such as within an ISR, for over 3.3 ms the UART ISR will not be run and characters will be lost, and although there is sufficient time to read all sensors within the time for one UART character other parts of the program may delay the running of either ISR. For this reason each sensor was read individually and a simple state machine (Figure 4.6) used to determine which sensor to read next. Each sensor would be read with the same time interval, but with a small offset between sensors.

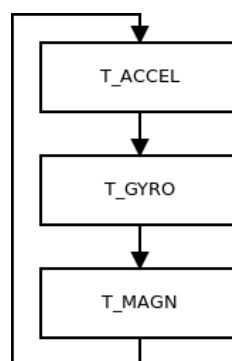


FIGURE 4.6: State Machine - Timed Commands / Reading of Sensors

The sensors were read every 15 ms (with the interrupt being called every 5 ms) to give a sample rate of 66.7 Hz. This was higher than the maximum sample rate of the magnetometer (50 Hz) and so no more gains from increasing sample rate could be achieved for heading control. The accelerometer and gyroscope had a greater sample rate but the same rate was used for all sensors to simplify the autopilot, with the ability to increase the sample rate later if necessary.

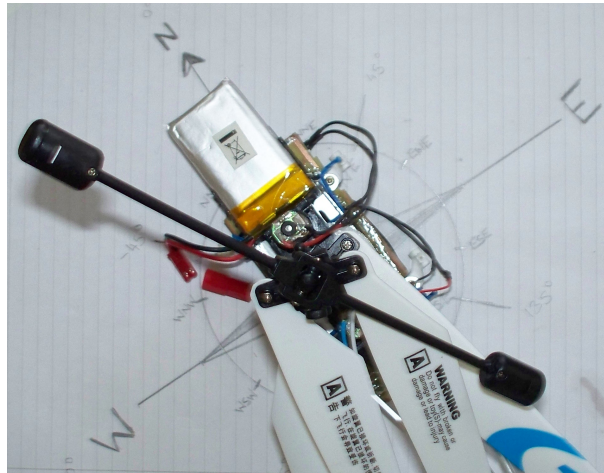


FIGURE 4.7: Calibration of magnetometer

Due to the positioning of the magnetometer and the motors, as shown in Appendix F, the magnetometer required calibration as the permanent magnets in the motors introduced a constant offset. Magnetometer readings were taken at the four cardinal directions in order to record minimum and maximum values for both the horizontal axes which could then be used to calculate the range and offset and normalise the data (Figure 4.8) using a similar method to Microchip application note 'AN996' [23]. The cardinal directions were indicated by a compass rose that was drawn up using a hand-held compass as a reference as shown in Figure 4.7. The magnetic field from the motors also caused the readings to overflow so the range had to be increased to ± 2.0 Ga to allow the heading to be calculated while reducing the gain as little as possible to keep higher resolution. The calibration data was stored in a C struct which could be saved to the AVR's EEPROM memory so it did not require re-calibration after the autopilot had been restarted. The code used to calibrate the magnetometer is shown in Listing G.4.

Although the offset introduced by the motors is constant while the motors are off and the helicopter is standing on the ground, the magnetic fields change once current is flowing through the motors. There is little that can be done to remove this effect and so inaccuracies will be introduced into heading control. Also, although the magnetometer provides three axes of data there is no tilt compensation performed

$$N_{range} = N_{max} - N_{min}$$

$$N_{offset} = \frac{N_{range}}{2} - N_{max}$$

$$Magn_{N(cal)} = \frac{(Magn_N + N_{offset}) \times 200}{N_{range}}$$

(Where 'N' represents the X or Y axis)

FIGURE 4.8: Calculations to normalise magnetometer readings

as the helicopter used will be unstable if the pitch or roll exceeds a few degrees. The stabiliser bar should prevent roll however the pitch PID controller will need to be able to prevent significant unintentional pitching movements.

4.7 PCB Design and Manufacture

All the circuit boards for the project were manufactured using the toner transfer method as described in [15] and [31]. Initially the plan was to split the autopilot across separate boards so that different parts of the autopilot could be redesigned and remade without having to remake the entire autopilot. This would also allow versions of each board to be designed to use both through-hole and surface components as available and needed. The through-hole version of the autopilot proved to be too heavy for the helicopter to be able to fly but it still provided a way to test the functionality of both the circuit design and the PCB design.

Different areas of the circuit board needed different voltages and so the design had to include voltage regulators to provide both 3.3 V (needed by digital components) and 5 V (needed for the RF receiver). As the helicopter's battery was only rated for 3.7 V the voltage had to be stepped-up for the wireless receiver which was not ideal but provided a way to use a simple and inexpensive wireless link as the majority of similar receivers also required a 5 V supply. A voltage divider was also needed to step-down the 5 V output of the wireless receiver to 3.3 V for the AVR's UART. Also, the AVR programmer used to program the autopilot used 5 V and so a method to disconnect the AVR from the rest of the circuit for programming had to be designed into the PCB. This was achieved by using a jumper to connect the AVR to the autopilot's 3.3 V supply which could also be used as a connection point for 5 V for programming.

The first testing that included driving the main motors of the helicopter used surface mount components and was split into two boards, one for the majority of the autopilot and one for motor control, provisions were made for power distribution but proved to be insufficient. The traces for the power supply were made as wide as possible so they could carry sufficient current and decoupling capacitors were added for each integrated circuit used. At a low PWM duty cycle little current would be drawn and the autopilot would function as expected but at a higher duty cycle, and therefore higher current, the power supply would not be sufficiently stable and this would be made apparent by the microcontroller resetting. Further investigation was therefore undertaken as to how to further decouple different areas of the autopilot.

4.7.1 Power Supply Decoupling

The circuitry for the autopilot is split into three main areas as shown in Table 4.1. Both the digital and motor control circuitry contribute ripple to the power supply, which reduces the accuracy of the sensors as they require a stable supply. The digital circuitry (the microcontroller) adds high frequency (8 MHz) but low magnitude spikes as it only draws current on the edge of the clock signal [7] while the motors will contribute a larger ripple but at the PWM frequency (3 kHz) which is lower than the microcontroller clock frequency. The large currents drawn by the motors at high PWM duty cycles caused ripple on the supply which exceeded the operating limits of the digital components. This meant that it was important to isolate the different areas of the autopilot as much as possible and the autopilot circuit board was redesigned with power distribution as a priority.

Area of Circuit	Requirements and Impacts
Analogue Circuitry (Sensors)	Very stable supply Low current draw Few spikes or ripple
Digital Circuitry	Relatively stable supply Current drawn in short spikes
Motor Control	No supply requirement High current draw in spikes

TABLE 4.1: Different areas of circuitry for autopilot

As the functionality of the basic circuits had been verified the autopilot was designed as a single board as it offered more opportunities for decoupling and reduced the overall weight. Due to earlier problems as much space as possible for decoupling

capacitors was added for each component, the autopilot could then be tested and further capacitors could be added later to help decoupling if needed. Decoupling was also added to the supply as described in Lattice technical note 'TN1068' [27] to provide power during short high current demands. Atmel application note 'AVR042' [7] states that in high noise situations the internal pull-up resistor on the \overline{RESET} pin may not be sufficient and so space was provided for an external pull-up resistor in case this proved to be a problem. Both TN1068 [27] and AVR042 [7] described the use of a low-pass filter (using an inductor and a capacitor) to improve the decoupling where there are significant current spikes. A low-pass filter was placed to isolate the supply to the motors from the supply to other components, a jumper was added to be able to bypass the low-pass filter for testing without driving the motors and to be able to observe if the filter had any impact on performance.

The power distribution for the circuit was designed in a star topology as this would help prevent noise and ripple from one component affecting other components [32]. As the circuit board was only a single-sided board it was not entirely possible to isolate the ground for each component but only the sensors and the wireless receiver directly shared a ground trace. Ideally two ground planes would be used, one for the motors and one for all other parts of the autopilot, as the use of a ground plane would assist in the decoupling of components while the high ripple caused by the motors would require a separate ground plane for further isolation. A circuit board using a ground plane was designed but was found to reduce the effectiveness of the toner transfer method as solid blocks of toner would not transfer well to copper clad board and so care was taken to design the ground distribution to compensate for the lack of a ground plane.

The original controller for the helicopter used resistors between the driving pins and the gates of the MOSFETs, this helps to reduce ringing caused by resonance within the gate drive circuit [30] and so resistors were added between the PWM outputs of the AVR and the gates of the MOSFETs. Once the design was otherwise finished as many extra connection points were added as there were space for to allow the autopilot to be extended, this also allowed easier debugging as a spare I/O pin could be used to output a signal to show the state of the autopilot.

4.8 PID Controller

Figure 4.9 shows the flow of the sensor data through the autopilot, the first step is to calculate the current attitude of the helicopter. The decision was made to treat

each axis (pitch, roll and yaw) independently as due to the particular design of helicopter a change in one axis will have very little effect on the other axes, this is because roll is fixed by the balance bar and so any horizontal translational motion is exclusively controlled by changes in the angle of pitch. This is in contrast to fixed-wing and other rotary-wing aircraft where both roll and pitch have an effect on horizontal motion.

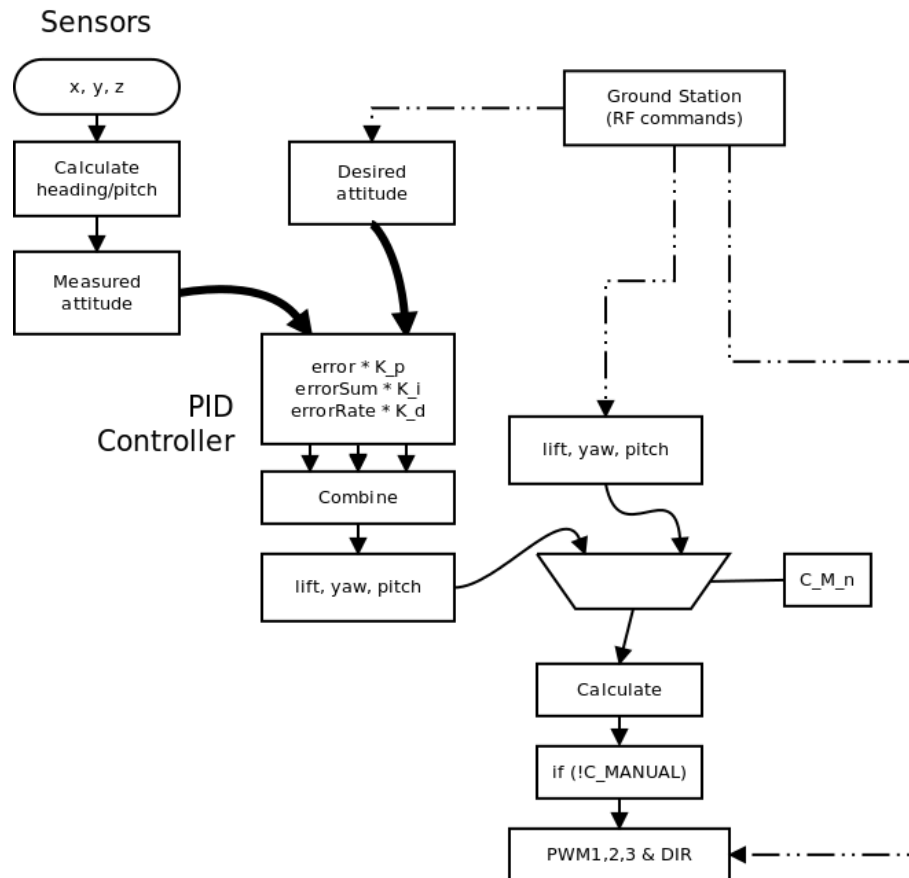


FIGURE 4.9: Flow of data through autopilot

Figure 4.10 shows the labelling of the sensor axes. The current angle of pitch could be measured using the accelerometer readings for the Z-X plane, the sensor would detect a constant acceleration of 1 g due to gravity which would always be directed downwards in the reference frame. By measuring the difference between the detected acceleration and the expected acceleration the angle of pitch could be determined. In a similar way, the Earth's magnetic field provided a reference for the angle of yaw and so the angle between the detected magnetic field in the magnetometer's X-Y plane (after calibration) and the expected field would give a value for the current heading of the helicopter.

Inverse trigonometric functions from the avr-libc library were used to calculate the angles. The calculated angles comprise the measured attitude which can then

be compared to the desired attitude so that the PID controller can calculate the correct restorative action to return the helicopter to the current desired attitude. Each calculation would be performed after the reading of the sensor but before the next sensor had been read. The time for an inverse trigonometric function was measured to be in the range $130 \mu s \rightarrow 240 \mu s$, or $1040 \rightarrow 1920$ cycles, although this would depend on the ease of calculation for the input values and is only a rough estimate but still shows the significant amount of processing time allocated to the calculation of angles.

The implementation of the PID controller was, in part, adapted from Atmel application note 'AVR221' [6]. The constants for the controller, as well as the cumulative sum of the error, were stored in a single data structure as shown in Listing G.2. The PID controller (Listing G.3) took the measured and desired values as well as the PID data structure and calculated the necessary motor output as well as updating the data structure with the new cumulative sum. This function also prevented the integral term from growing too large by limiting the magnitude of the cumulative error. The derivative term of the controller was directly taken from the gyroscope as this provided a way to benefit from the quicker response of the gyroscope without implementing Kalman filtering to combine sensor data which would increase the complexity of the autopilot. Also, if the derivative term was based on the calculated rate of change of the error then any changes in the desired attitude would result in “an unwanted rapid change in the control input” (AVR221 [6]).

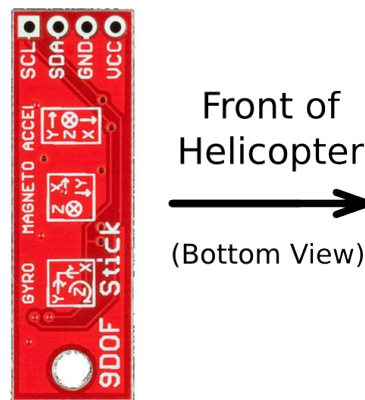


FIGURE 4.10: Orientation of sensor stick with respect to helicopter (from [28])

The same code for the PID controller could be used to control both the pitch and the heading of the helicopter by changing the sensor data passed to the controller, simplifying the implementation. The output of the PID controllers was combined into data for the 'calculated' control mode and so it was possible to enable or disable

each PID controller separately using the control register to allow individual testing while the other axes were controlled manually.

4.9 Environment Mapping

The sensors used for environment mapping were ultrasonic distance sensors produced by Maxbotix [20]. By combining the data known about the position of the helicopter with distance readings it is possible to build up an image of the surrounding environment. Also, the distance gives an indication of the linear position of the helicopter relative to its environment and so helps to locate the helicopter in space.

The sensors provided multiple ways to read the distance data, and in this case the analogue output was read by the AVR's ADC. The C_ADC bit in the control register controlled if the ADC was currently taking readings or not. As with other data, the readings were read from the ADC in an ISR into a global variable. The distance readings did not require any processing and so no provision was made to indicate the presence of new distance data using the status register. Also, a command was added to the communications protocol to allow the distance data to be saved to EEPROM for later analysis.

5. System Testing and Results

The basic functionality of each part of the autopilot was tested during prototyping to verify its operation, the functionality was further checked once the system was more assembled so that the interaction between parts of the system could also be verified.

5.1 Power Supply

After the multiple board version of the autopilot had problems with decoupling the first area of the single board version to be tested was the power supply and decoupling between different areas of the board. The design had multiple points where the supply rails could be disconnected so the ripple and spikes caused by the motors could be observed without any possibility of damaging other components. A signal generator was used to apply a signal to the gate of the MOSFET which was equivalent to the PWM that would be applied by the AVR. The positive supply rail was then observed (shown in Figure 5.1) showing that the motors, when driven, introduced significant ripple to the supply as well as short spikes at the start and end of each pulse to the gate, this was observed before any decoupling capacitors were added to the board to provide a reference for the effect that the additional decoupling efforts had.

After additional decoupling capacitors were added to the autopilot the supply was then measured in the same way as before and it was observed that significant ripple was still present on the digital supply as well as short spikes. An inductor was therefore added between the supply to the motors and the supply to the digital circuitry to further reduce the spikes. Figure 5.2 shows an close-up view of the effect that the low-pass filter had on the spikes on the supply. The maximum voltage now reached is ≈ 4.7 V which is within the limits of other components and is significantly less than the spikes shown in Figure 5.1 which in some cases had a magnitude of over 7 V, although the exact magnitude of the spikes was difficult to determine due to their short duration. These spikes were due to flyback from the motors, so it appeared that the protection diodes used were insufficient as they did not appear to react sufficiently quickly to entirely remove the voltage spike despite having an almost identical rating to the diodes used for the original controller of

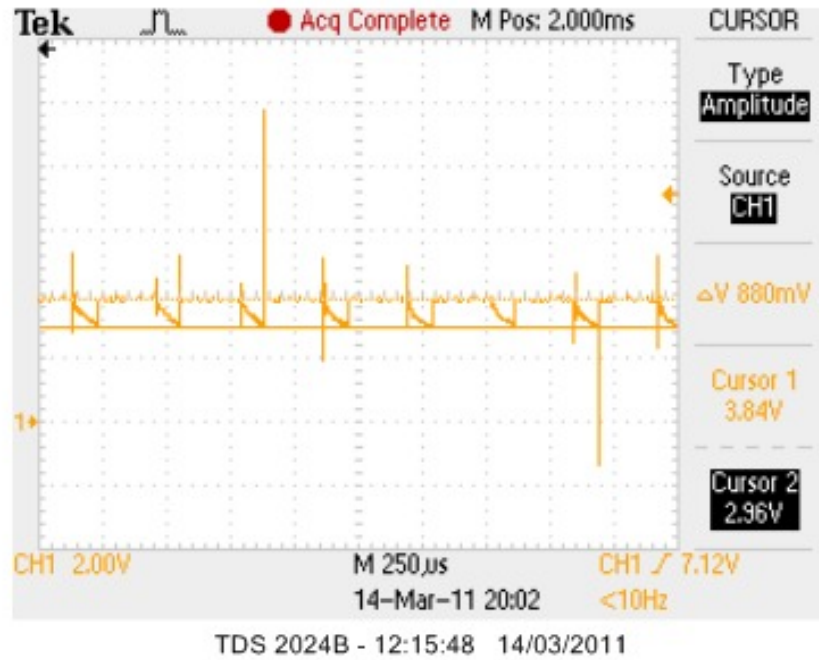


FIGURE 5.1: Positive supply rail measured at motor

the helicopter. After the low pass filter had been added, however, the spikes were reduced to sufficiently low levels as to not cause further problems. Also, the pull-up resistor for the \overline{RESET} pin was not needed as the isolation between parts of the autopilot proved sufficient.



FIGURE 5.2: Positive supply rail measured at digital supply (with additional decoupling)

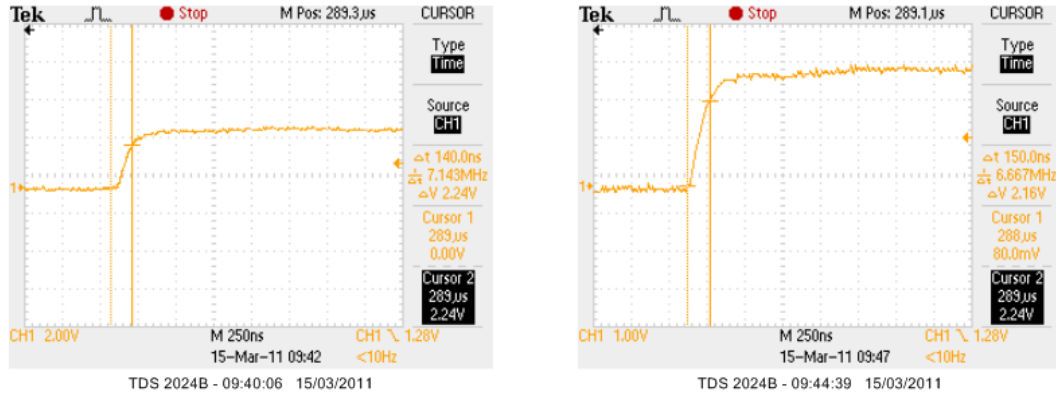
The signal at the gate of the MOSFET was observed to confirm that the gate resistor had no impact. Figure 5.4 shows a comparison of the PWM signal being applied directly and through the gate resistor. The rise time increased slightly from 140 ns to 150 ns but there was little overall impact, also, 150 ns is a small proportion of the PWM period of 320 μ s.

The time constant for the RC circuit formed by the gate resistor and gate capacitance was calculated for both the original controller and the autopilot as shown in Figure 5.3. This shows that the time constant is less for the autopilot and so, although other parts of the original controller's drive circuit are unknown, the autopilot should be able to sufficiently drive the MOSFET gate.

$$\tau = RC = 330\Omega \times 1000pF = 330ns \quad \tau = RC = 10\Omega \times 1350pF = 13.5ns$$

(a) Original Controller
(b) Autopilot

FIGURE 5.3: MOSFET gate RC time constant



(a) PWM signal applied directly to gate (140 ns)

(b) PWM signal applied through resistor (150 ns)

FIGURE 5.4: MOSFET gate rise time

Each of the different voltage rails were also tested to check that they were able to provide a stable supply at the correct voltage. This made sure that while the autopilot was operating all parts of the circuit would still function correctly. Although the decoupling did not stop all ripple on the power supply the use of voltage regulators prevent the ripple being present on the supply to the digital components.

The final version of the PCB used copper clad board with a thin substrate which reduced the overall weight of the autopilot. The thinness of the board meant it was flexible, which resulted in bad solder joints at the MOSFETs used to control the motors. This meant that occasionally the board would require flexing for the motors to be turned on.

The weight of the helicopter was measured in its original form and also with the autopilot to compare the difference. The original weight of the helicopter was 140 g which was less than the weight with the autopilot (at 143 g), however, being designed as a toy remote control helicopter there was an amount of material that had solely aesthetic purpose and so could be removed to reduce the weight. This allowed the total weight of the system to be reduced to 135 g, less than the original weight.

5.2 Remote Control

The wireless communications required testing to ensure that there was sufficient synchronisation between the transmitter and the receiver for a reliable communications link. Figure 5.5 shows the improvement achieved when both framing and continuous transmission were used for the communications link, the pulses are much more defined and so it is more likely that they will be correctly read by the UART on the AVR. While commands could be received by the autopilot without framing it was not sufficiently reliable, especially to provide remote control of the helicopter in flight, as most of the time the commands would be received incorrectly. Framing provided sufficient reliability that the parity, and other validation provisions within the protocol, did not need to be implemented.

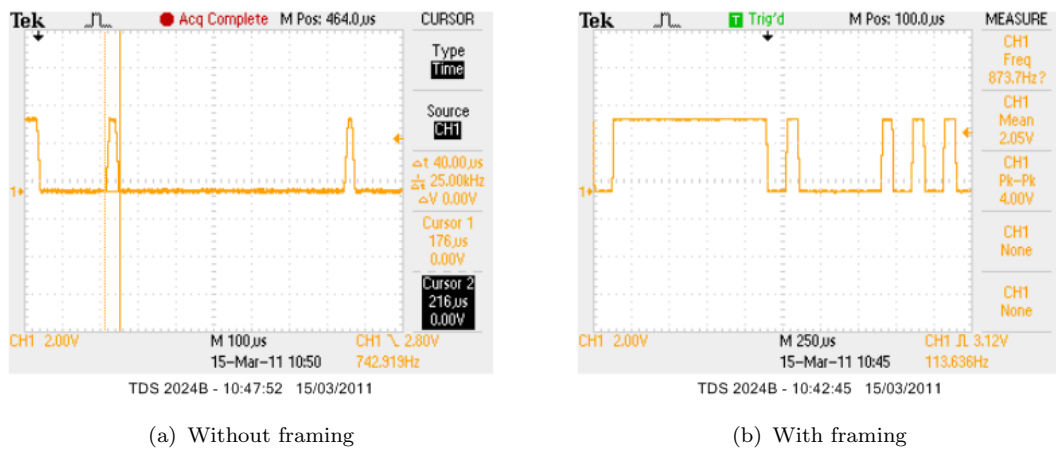


FIGURE 5.5: Effect of framing on RF receiver synchronisation

Once reliable communications were possible between the autopilot and the ground station the joystick control mode of the helicopter was tested. The first flight test of the helicopter showed a constant yawing motion present when both main rotors were driven at the same PWM duty cycle. This was because the balance bar meant

that the characteristics of both rotors were different, resulting in different speeds when driven by the same amount. The difference in speed caused a resultant torque and so a yawing motion. This rotation around the vertical axis could have been corrected by introducing an offset into the yaw calculations but would be corrected by the controller once implemented.

The remote control showed that control of the helicopter was possible with updates sent to the motors every 115 ms, an update rate of 8.7 Hz. However, it was evident that this was near the lower limit of the update rate as the delay in response to inputs could be observed while flying the helicopter, making control more difficult. The PID controller would be unable to make the same corrections possible with manual control so it would probably require a quicker update rate to successfully stabilise the helicopter but gave a rough upper limit to the time between motor updates. As the sensors were read, and the necessary calculations performed, at a rate of 66.7 Hz the update rate should be sufficiently high to allow satisfactory PID control.

5.3 PID Tuning

The design of the helicopter meant that each axis of rotation had little impact on other axes and so each PID controller only had to control one axis. This independence also meant that the testing and tuning of each PID controller could occur separately.

5.3.1 Pitch Control

For flight the helicopter is supported by lift generated by the main rotors and so by suspending the helicopter at a central point the dynamics of the pitch axis could be investigated in a consistent and reliable fashion while giving the same characteristics as during flight. By being placed in a fixed position the angle of pitch could be measured by video by putting a backdrop with angles marked as a reference (Figure 5.6). The pitch axis is inherently stable as the weight of the helicopter will return the pitch axis to a fixed angle however a quicker response was required to prevent unwanted movement forwards and backwards. Also, pitch control is necessary to achieve controlled movement.

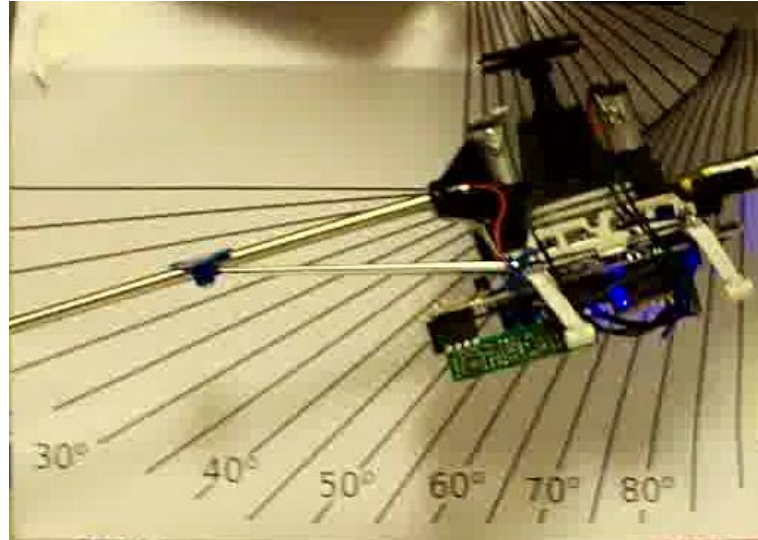


FIGURE 5.6: Pitch PID tuning setup

The measurements were made by pushing the pitch axis to an offset of 20° , greater than any disturbance that should be encountered in flight but would make measurement easier, and recording the resultant motion when released. The number of frames from the start to a maximum oscillation of 5° were counted to give a value for the settling time. To provide a control, four videos were taken with the motors off. The autopilot was then used to control the pitch axis and the ground station used to change the PID constants between tests. Each controller constant was changed independently so its effect could be observed to help direct the tuning.

Proportional control appeared to reduce the stability of the pitch axis, increasing the settling time from ≈ 6.3 s to ≈ 17.9 s, this showed that a P controller was insufficient and so the derivative and integral terms were necessary. The derivative term rapidly improved the dynamic response of the helicopter, eventually reducing the settling time to 0.8 s, but further increases did not result in any changes to the characteristics. Adding a small amount of integral control removed the steady state error present without having any apparent effect on the settling time, however, increasing the integral term resulted in a deterioration of the dynamic response.

PID constants of $K_p = 15$, $K_i = 1$ and $K_d = 100$ gave a settling time of ≈ 0.8 s. While this is a significant amount of time to take to return to the desired attitude it is the result of an initial displacement of 20° which is very unlikely to be encountered in normal flying conditions. The tail rotor did not appear to be powerful enough to improve on this response as it had to overcome the inertia of the helicopter.

5.3.2 Heading Control

Testing of the heading PID controller was more difficult than the pitch control, as any method of suspending the helicopter would introduce friction and so change the system dynamics. The testing method used was to change the constants while the helicopter was landed and then to use the remote control to briefly fly the helicopter, observing the resulting stability. Control of pitch was given to the PID controller as it was demonstrated that it could provide stable control. The judgement of the stability was mainly subjective but a few objective observations could be made, increasing the proportional or derivative terms too far would result in overshoot and ringing which was visible as rapid oscillations in the heading. The removal of ringing showed an objective improvement in the heading control but other changes to the constants had little noticeable effect on the dynamic response, reducing the opportunities for further optimising the controller. Values of $K_p = 1$, $K_i = 1$ and $K_d = 10$ appeared to give stable control of the heading without causing ringing.

5.4 Environment Mapping

For the initial testing of the autopilots environment mapping capabilities the helicopter was suspended in the middle of a room and allowed to turn freely about the yaw axis. As the helicopter was rotated, readings from the distance sensor, as well as the current heading, were saved into the AVR's EEPROM memory. Once a number of readings had been taken the data was retrieved and plotted to give an image of the surroundings as sensed by the autopilot. Figure 5.7 shows the results that were obtained. As it was only an initial test, no efforts were made to ensure equal spacing of the readings and so some areas didn't have any data obtained. The data did show the outline of the room but due to apparent noise in the measurements the distances to the walls varied by about a metre. The resulting graph shows the need for averaging or further filtering of the data to give a useful model of the helicopters surroundings. Although the readings taken were not acquired while the helicopter was in flight the same methodology could be applied.

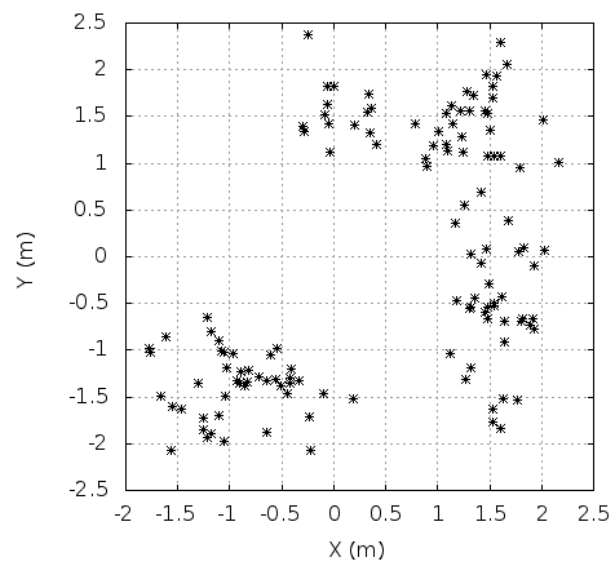


FIGURE 5.7: Environment Mapping - Initial Test

6. Evaluation

6.1 Fulfilment of Scope

- Control of helicopter by microcontroller

The autopilot was able to fully control the three motors of the chosen helicopter, providing speed control to all motors. The tail motor could also be driven in both directions, necessary to fully control the pitch of the helicopter and so provide control of forwards and backwards motion. Different control modes of the motors were implemented, allowing both on-board control and remote control for different purposes.

- Communication between the helicopter and a ground station

A communications link was implemented between the ground station and the autopilot, however, it was only able to send commands to the autopilot. A two-way connection was not needed as if data was needed from the autopilot it is possible to temporarily create a wired link, or save the information to the on-board EEPROM memory for later retrieval. This did make it more difficult to observe the internal state of the autopilot, but for specific testing the motors could be used to show a certain state.

In order to fully achieve the goal of communication between the helicopter and a ground station a wireless transceiver would be required which would be more complex than the wireless transmitter and receiver pair used for the system. The provisions made to allow two-way communications only gave a temporary link, however, it was decided that the one-way communications link was more in-line with the overall goals of the project as it offered a potential way to reduce weight and cost of the autopilot.

- Attitude determination and stabilisation

It was possible to determine the full attitude of the helicopter completely from the sensor data but the autopilot only calculated the angles of pitch and yaw. This was because the roll angle was not needed for stable flight and so processing power could be saved by not calculating it.

A PID controller that compared the measured attitude with the desired attitude was used to stabilise the helicopter. After tuning of the controller it

gave stable control of both the pitch and yaw axes and changing the desired attitude resulted in controlled movement of the autopilot and helicopter.

- Environment mapping

Little of the environment mapping functionality of the autopilot was implemented due to problems encountered with earlier functionality. Readings from a distance sensor allowed basic observation of the surroundings but further work was still required to produce useful data and better integrate the functionality into the rest of the autopilot software.

6.2 Project Management

Figure 6.1 shows the differences between the planned schedule of the project and the actual work done. The main delay was caused by the problems due to insufficient power supply decoupling with the multiple board version of the autopilot. In order to solve the problems with the overall design that this highlighted more time was required to reassess the design of the component parts of the autopilot. Extra time had been allocated to the design and implementation of the controller to stabilise the helicopter and so this time could instead be used to solve the problems with the power supply. Fixing the power distribution required the redesign of the autopilot circuit board and so took more time than the extra allocated. After work on stable flight was completed there was insufficient time to fully complete the environment mapping functionality and so the focus was changed to get a basic implementation working so that even if not fully functional the methodology could be evaluated.

6.3 Further Work

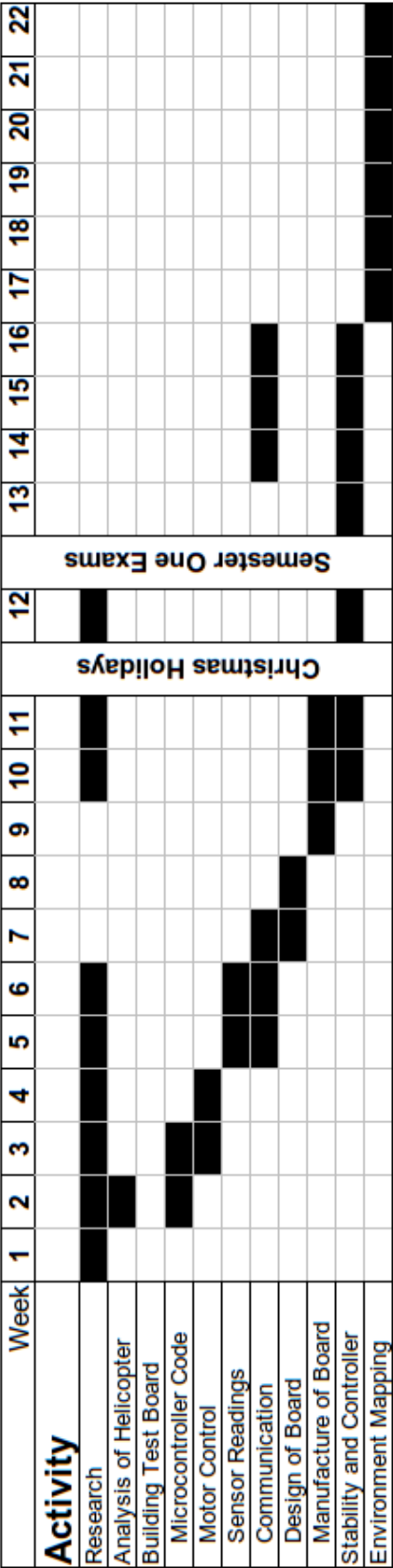
There were some methods that could have been used to improve the autopilot using the hardware developed. Although provisions were made for checking the validity of commands, the communications link did not fully implement them as they were not needed for a reliable connection. The protocol included bytes that could be used for the data byte count and parity but not were used in software. The addition of these features would further increase the reliability of communications between the ground station and autopilot which would potentially increase the usable range of the link.

The speed at which the sensors were read and the controller reacted could also be improved with the existing hardware used. The I²C protocol allows for multiple speeds of operation, commonly the 100 kHz 'standard mode' and the 400 kHz 'fast mode' [25]. The standard mode was used for the project as the fast mode would be less noise resistant and so would require further testing to determine if the sensors could be read reliably in flight. If the sensors were read more quickly they could be read more often and so the values sent to the motors could be updated more quickly. Increasing the sample rate would improve the ability of the autopilot to deal with high frequency dynamics. Also, with the current design of the software the sensors were read within the interrupt service routine and so speeding up the communications would reduce the time spent in the ISR. This would improve the autopilot as it would increase the time that it was capable of responding to other interrupts. The communications protocol could also be adapted to provide quicker communications, the implementation uses a certain amount of overhead to provide reliability but the use of parity or Manchester encoding could reduce this overhead without sacrificing reliability.

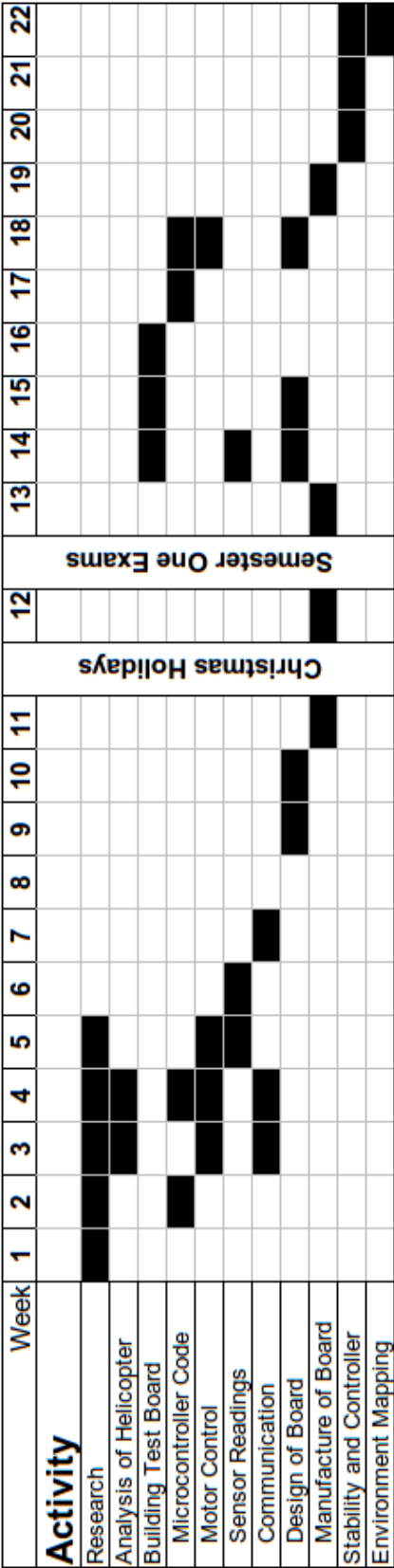
Also, the design of the helicopter allowed for additional hardware to be added to extend the functionality without major changes. Connection points to the ADC of the AVR were left available, this meant that battery voltage detection could be easily implemented. Using a voltage divider to scale down the battery voltage, it could be connected to the AVR and so be acted upon by the autopilot, for example, to enact a graceful landing when the supply drops too low to sustain flight.

Further work was also needed on the environment mapping functionality, including investigating how best to process the data to improve the quality of the model of the surroundings. Extending this functionality to give the autopilot data about the helicopters linear position would help to provide a means for greater autonomy.

Using system identification techniques to model the helicopter would also help improve the system. If a model of the dynamics of the helicopter was known then the PID controller could be directly designed for the actual dynamics of the system and so improve the response more accurately than manual tuning could. An improved dynamic response would increase the stability of the helicopter and so also its usefulness in some applications.



(a) Gantt Chart of Planned Work



(b) Gantt Chart Record of Work Done

FIGURE 6.1: Gantt Charts

7. Conclusion

The final version of the autopilot was limited in its capability for autonomous control, it was able to stabilise itself in mid-air but due to the lack of progress made towards the environment mapping functionality the autopilot had limited knowledge of its linear position. For example, this meant that the height of the helicopter had to be manually controlled during testing. Despite the lack of autonomous behaviour sufficient progress was made with the project to show the capabilities and limitations of a rotary-wing aerial vehicle utilising mechanical stabilisation. Had the issues with decoupling been sufficiently dealt with in the initial design then more time would have been available to fully integrate the distance sensors with the autopilot. This would potentially have allowed greater autonomy by the autopilot, such as a short program capable of taking off and surveying a room.

The project showed that it would be possible to use mechanical stabilisation to construct an inexpensive aerial vehicle. The biggest limitation was the carrying capability of the chosen helicopter, which was sufficient to carry the autopilot but did not have spare capacity for much more instrumentation to further increase the functionality. The same techniques could be used to produce an autopilot for a helicopter with greater carrying capacity, for example the E-Sky Lama series [12] which uses the same form of mechanical stabilisation, to allow more functionality. Also, the maximum length of each flight was limited by the capacity of the battery but this could again be solved by applying the same techniques to a different model of helicopter.

One of the limitations with the general design was that the mechanical stabilisation prevented control of the roll axis and so the autopilot would not be able to correct for small lateral movements without rotating before making a corrective motion. If the position of the helicopter is known then this limitation can be compensated for but reduces the usefulness where precise positioning is required.

For this project an existing remote control helicopter was adapted as it allowed the focus to be placed on the electronic control of the helicopter rather than manufacturing and testing of the helicopter itself. The use of a consumer RC helicopter saves time on the development of the airframe but the same technique of mechanical stabilisation could be used to produce a bespoke helicopter which could then better suit the intended application. A construction of a custom-made system would

be more expensive and so the increased complexity of an autopilot with electronic control of all axes may make a smaller contribution to the total cost of the system, reducing the need for mechanical stabilisation.

The total cost of the prototype autopilot developed was £128.43 (as shown in Appendix H), this is less expensive than other solutions that could be used to provide a stable aerial platform, such as XAircraft quadcopters [33] which range from a cost of about £300 to £500. A mechanically stabilised system requires less hardware and so can be manufactured at a lower cost, although a quadcopter or other rotary-wing vehicles would provide more control. For some applications precise control would not be as necessary and so the reduced cost would be a suitable trade-off. A more inexpensive system would also allow aerial remote sensing for some applications where the cost of more complex systems was prohibitive.

A. Original Project Brief

A.1 Problem

In the modern world there are many situations which could benefit from the use of autonomous aerial vehicle platforms, mainly those that involve remote sensing such as investigating distant or dangerous environments. The main problem with these platforms is the cost involved which makes their use overly expensive for some applications which could otherwise benefit. Recently there have been an increased number of inexpensive remote control helicopters sold as toys due to advances in the field which simplify the stabilisation. The aim of the project is to adapt a consumer remote control helicopter to allow autonomous control, in order to provide an inexpensive platform for applications which require or could benefit from an autonomous aerial vehicle.

A.2 Goals and Scope

- Implement microprocessor control of the chosen RC helicopter
- Use sensors to determine the attitude of the helicopter
 - Control the helicopter through the use of the microprocessor and sensors to allow hovering and controlled movement utilizing control theory to construct a robust controller.
- Use a proximity sensor to map the helicopters environment
 - Automatically map out the helicopters surroundings and build up a model of the room using signal processing to improve the accuracy of the model.
- Communication between the helicopter and a ground station
 - Implement a communications protocol that allows control by a ground station and returns any collected data using communications theory to give a reliable link.

B. Autopilot Registers

The contents of the autopilot's status and control registers are shown in Table B.1. On an interrupt the ISR would set the relevant bit in the status register. The state machine would stay in an idle state until the status register signified the presence of new sensor data (S_DATA) or data from the UART (S_UART), at this point it would perform any relevant processing before clearing the status bit, allowing the storage of new data. An intermediate stage was added to the processing of commands as shown in Figure 4.1 so any incoming commands would be stored in a buffer, this allowed the command to be checked for validity before it was processed. It also allowed any commands generated from within the program to be run concurrently with commands received from the ground station by providing memory for two commands simultaneously, the presence of the command could then be indicated by setting the S_COMMAND bit once the intended command had been set. This also had the added benefit of reducing time spent in the ST_COMMAND and ST_UART_PROC states which would allow new sensor data to be processed quicker as the PID controller relies somewhat on the sensors being sampled at a consistent rate.

Status Register		
Bit	Name	Indicates
6	S_D_MAGN	Magnetometer data read
5	S_D_GYRO	Gyroscope data read
4	S_D_ACCEL	Accelerometer data read
3	S_D_OVF	Data Overflow
2	S_DATA	New sensor data available
1	S_COMMAND	New command available
0	S_UART	New data from UART

Control Register		
Bit	Name	Function (Set/Cleared)
5	C_ADC	Enable/disable ADC
4	C_M_PITCH	Ground station/PID control of pitch
3	C_M_YAW	Ground station/PID control of yaw/heading
2	C_M_LIFT	Ground station/PID control of lift/height
1	C_DEBUG	Enable/disable debugging information
0	C_MANUAL	Direct/Calculated control of motors

TABLE B.1: Status and Control Registers

C. Communications Protocol

The communications protocol was inspired by the ArduPilot Communications Protocol [5] and consisted of a preamble, 2-byte command, a byte specifying data length and the data itself. The preamble is the character '!' (ASCII 0x21) followed by a two letter command as specified in Appendix D. The data and its length was then followed with a new line character (ASCII 0x0A) to specify the end of the command.

The protocol was slightly changed for the wireless link to compensate for the reduced reliability. The packet length was now fixed to 8 bytes to prevent problems that would be encountered if a stop byte was not correctly received. Also, fixing the length of the commands simplified the use of a buffer to store the commands until they had been processed. The stop byte was replaced with a parity byte so that some form of verification could be performed on the received command but this was not required for a reliable link and so was not fully implemented. The final format is shown in Table C.1.

Framing was added around each byte of the command to help improve the synchronisation between the transmitter and receiver by ensuring a minimum number of transitions. The framing consisted of a 'U' (ASCII 0x55) and an 'A' (ASCII 0x41) followed by the byte of the command,

Byte	Use
0	Start Byte '!'
1	Command MSB
2	Command LSB
3	Data Byte Count
4	Data Byte 0
5	Data Byte 1
6	Data Byte 2
7	Parity Byte

TABLE C.1: Communications Protocol Format

D. Communications Protocol Commands

Table D.1 shows the listing of commands in the communications protocol used.

Byte 1	Byte 2	Command
c	M/m	Set/Clear C_MANUAL Direct/Calculated control of motors
	D/d	Set/Clear C_DEBUG Enables debug output on specified events
	L/l	Set/Clear C_M_LIFT Ground station/PID control of lift/height
	Y/y	Set/Clear C_M_YAW Ground station/PID control of yaw/heading
	P/p	Set/Clear C_M_PITCH Ground station/PID control of pitch
e	s	Save distance reading to EEPROM
I	a	Confirm accelerometer device id
	g	Confirm gyroscope device id
	m	Confirm magnetometer device id
m	N/E/S/W	Take N/E/S/W magnetometer reading
	U	Recalculate magnetometer calibration
	r	Load calibration data from EEPROM
	s	Save calibration data to EEPROM
p	p	Set pitch PID constants
	P/Q	Save/load pitch PID constants (EEPROM)
	q	Reset pitch PID controller
	y	Set yaw PID constants
	Y/Z	Save/load yaw PID constants (EEPROM)
s	z	Reset yaw PID controller
	A/a	Set all PWM channels (with tail up/down)
	D	Set desired attitude
	H	Set values for calculated control mode
	M	Set main rotor speed
	S	Set secondary rotor speed
	T	Set tail rotor speed
	t	Set tail rotor direction

TABLE D.1: Commands in the communications protocol

Figure E.1, Figure E.2 and Figure E.3 show the circuit schematic of the autopilot. Figure E.4 shows the final design of the circuit board used.

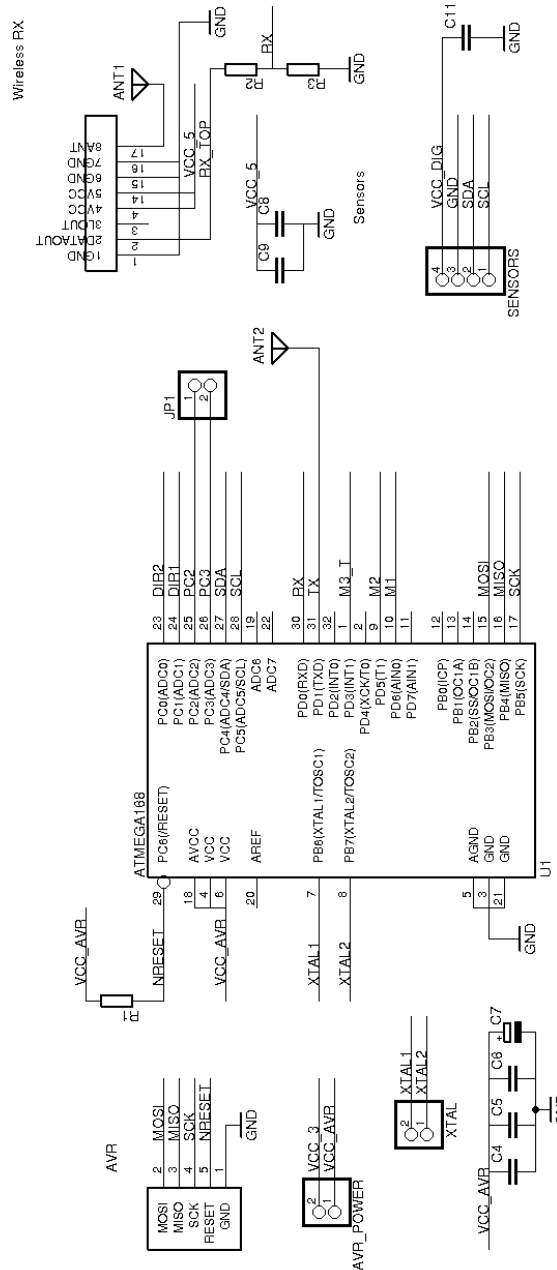


FIGURE E.1: Circuit Schematic - AVR

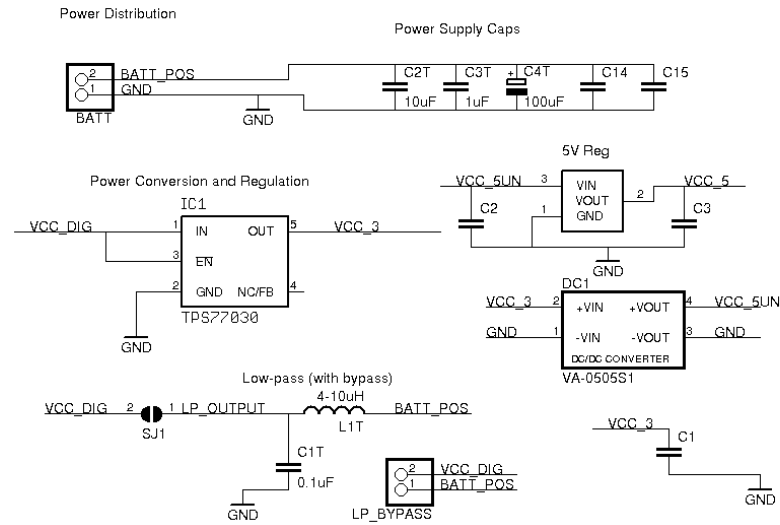


FIGURE E.2: Circuit Schematic - Power Distribution

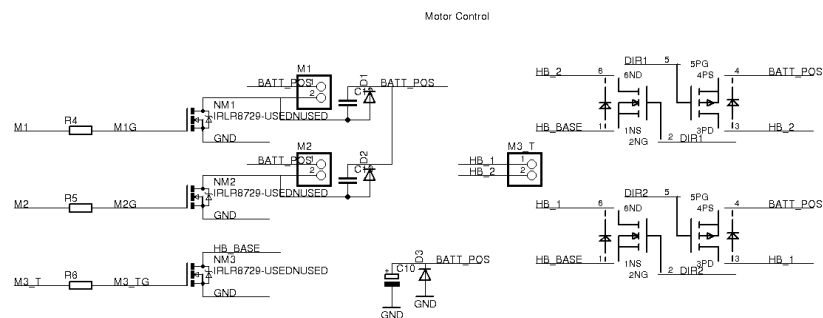


FIGURE E.3: Circuit Schematic - Motors

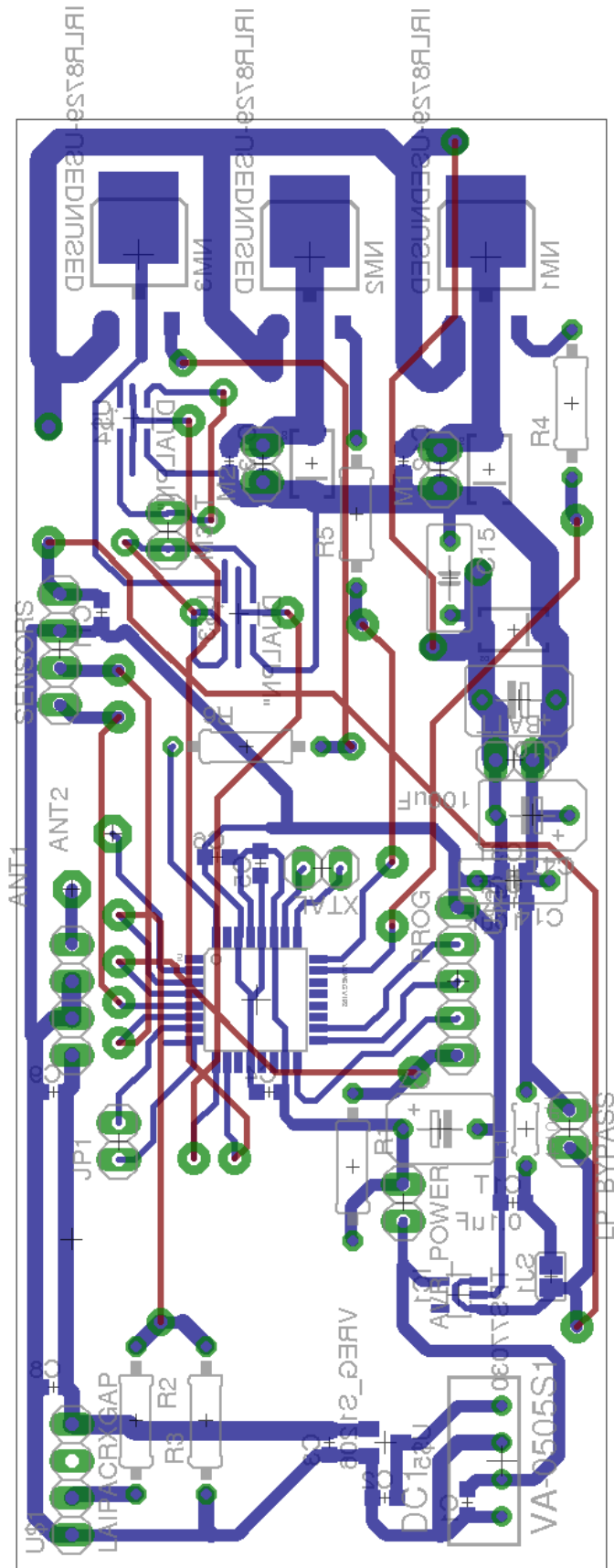


FIGURE E.4: Circuit Schematic - PCB

F. Helicopter Diagram

Figure F.1 shows a diagram of the helicopter used and where the autopilot is attached. Figure F.2 shows the same view of the system photographically.

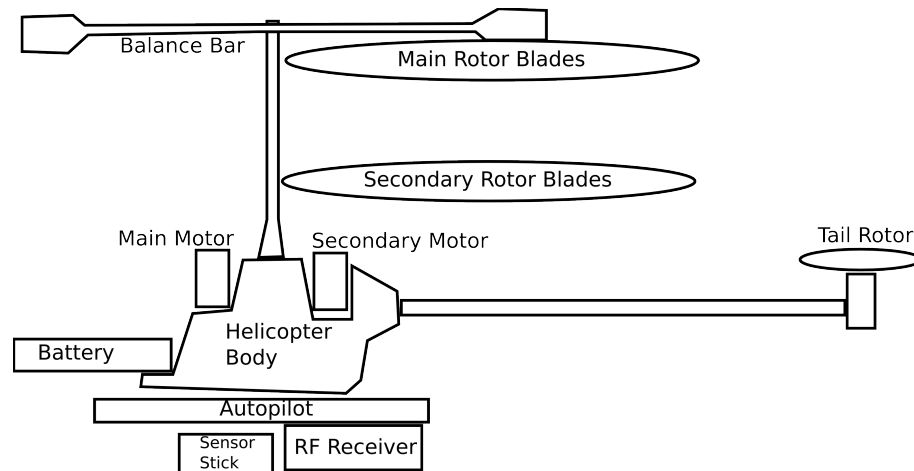


FIGURE F.1: Helicopter Diagram



FIGURE F.2: Helicopter Photograph

G. Code Listings

This appendix contains listings of source code that are relevant to explain certain functionality of the autopilot, the full source code is contained in Appendix I.

```
#define s_chk(V) (status & (V))
#define s_set(V) status = status | (V)
#define s_clr(V) status = status & ~(V)
#define c_chk(V) (control & (V))
#define c_set(V) control = control | (V)
#define c_clr(V) control = control & ~(V)

volatile unsigned char status, control;
```

LISTING G.1: Macros used to access status and control registers

```
typedef struct pid {
    uint8_t k_p, k_i, k_d; // Constants for PID
    float errorSum;        // Cumulative sum of error for integral term
} pid_t;
```

LISTING G.2: PID data structure

```
int16_t pid_process(pid_t* pid, int16_t measured,
                    int16_t setpoint, int16_t processRate)
{
    int16_t ret_val;
    int16_t error;

    error = setpoint - measured;
    // Cumulative sum disabled when integral term is zero
    // to prevent a sudden change in motor input
    if (pid->k_i != 0) {
        pid->errorSum += (error / 1.0);
    }

    if (pid->errorSum > MAX_I_TERM) pid->errorSum = MAX_I_TERM;
    if (pid->errorSum < MIN_I_TERM) pid->errorSum = MIN_I_TERM;

    int16_t eSumT, pRateT;

    // Both the errorSum and processRate need to be suitably
    // scaled as PID constants are limited to a range of 0-255
    eSumT = (int16_t)(pid->errorSum / 10.0);
    pRateT = (int16_t)(processRate / 100.0);

    ret_val = (error * pid->k_p) + (eSumT * pid->k_i) + (pRateT * pid->k_d);

    return ret_val;
}
```

LISTING G.3: PID processing function

```

void calc_magn_ref(sensor_ref_t* magn_ref)
{
    // Calculate offset and range from calibration data
    magn_ref->x_range = magn_ref->x_max - magn_ref->x_min;
    magn_ref->y_range = magn_ref->y_max - magn_ref->y_min;

    magn_ref->x_offset = (magn_ref->x_range / 2) - magn_ref->x_max;
    magn_ref->y_offset = (magn_ref->y_range / 2) - magn_ref->y_max;
}

sensor_data_t calc_magn_c(sensor_data_t magn, sensor_ref_t magn_ref)
{
    // Use the magnetometer range and offset to normalise heading data
    sensor_data_t magn_c;
    double temp;

    temp = ((double)magn.x) + ((double)magn_ref.x_offset);
    temp *= 200.0;
    temp = temp / ((double)magn_ref.x_range);

    magn_c.x = temp;

    temp = ((double)magn.y) + ((double)magn_ref.y_offset);
    temp *= 200.0;
    temp = temp / ((double)magn_ref.y_range);

    magn_c.y = temp;

    magn_c.z = 0;    // Z-axis is not used and so set to zero

    return magn_c;
}

```

LISTING G.4: Magnetometer calibration

```

void calc_pwm(controller_action_t controller_pc,
               controller_action_t controller_pid, volatile unsigned char control)
{
    controller_action_t controller_temp;
    int16_t p1, p2, p3;

    controller_temp = controller_mux(controller_pc, controller_pid, control);

    p1 = (int16_t)controller_temp.lift + (int16_t)controller_temp.yaw;
    p2 = (int16_t)controller_temp.lift - (int16_t)controller_temp.yaw;
    p3 = abs(controller_temp.pitch);

    // Min and max values
    if (p1 > 255) p1 = 255;
    if (p1 < 0) p1 = 0;

    if (p2 > 255) p2 = 255;
    if (p2 < 0) p2 = 0;

    if (p3 > 200) p3 = 200;
    if (p3 < 0) p3 = 0;
}

```

```
    Set_PWM1(p1);
    Set_PWM2(p2);
    Set_PWM3(p3);

    if (controller_temp.pitch > 0) {
        Set_PWM3_Dir(2);
    } else {
        Set_PWM3_Dir(1);
    }
}
```

LISTING G.5: Calculated mode of motor control

H. Costing

Table H.1 shows the cost of the autopilot prototype. If the autopilot was to be batch or mass produced then the PCB would be produced commercially as the toner transfer method would be too time consuming for volume production. The cost per board for a batch of 50 circuit boards would be about £4.60 and so would have little impact on the overall cost compared to the prototype.

<i>Item</i>	<i>Part</i>	<i>Qty</i>	<i>Cost</i>	
			<i>Unit</i>	<i>Subtotal</i>
Helicopter ¹	N04HN (Maplin)	1	£40.00	£40.00
PCB Copper Clad Board	1643092 (Farnell)	1	£2.75	£2.75
MOSFET N-Channel	IRLR8729	3	£0.38	£1.14
MOSFET Dual-PN	QS6M4TR	2	£0.10	£0.20
3.3V Voltage Regulator	TPS73033	1	£0.26	£0.26
5V Voltage Regulator	S-1206B50-M3T1G	1	£0.16	£0.16
DC-DC Boost Converter	IE0305S-H	1	£4.75	£4.75
AVR Microcontroller	Atmega168PA	1	£2.17	£2.17
Schottky Diodes	SS14	3	£0.09	£0.27
Assorted Passive Components ²	<i>n/a</i>	1	£0.50	£0.50
RF Rx/Tx Pair	RLP434 and TLP434	1	£5.75	£5.75
Accelerometer ³	ADXL345	1	£3.26	£3.26
Gyroscope ³	ITG-3200	1	£16.38	£16.38
Magnetometer ³	HMC5843	1	£30.44	£30.44
Ultrasonic Distance Sensor	LV-EZ0	1	£20.40	£20.40
			Total	£128.43

TABLE H.1: Costing of autopilot prototype

¹Cost of helicopter when purchased, current price is £60

²Approximate cost for resistors and capacitors, cost would be reduced for volume production

³Included on the Sparkfun SEN-10321 Sensor Stick [28]

I. CD Table of Contents

Autopilot\

main.c Source code of the autopilot software

compile.sh Shell script used to compile the autopilot software

c_program.sh Shell script used to program the autopilot

read_eeprom.sh Shell script to retrieve EEPROM memory

Other files comprise the remainder of the source code

Ground Station\

main.cpp Source code of the user interface

compile.sh Shell script used to compile the ground station software

Other files comprise the remainder of the source code

Results\

Environment Mapping\

results.xls Spreadsheet of results obtained from the distance sensor.

PID Tuning\

Recordings of the results from PID tuning. Subfolders are named according to the format “[K_p]-[K_i]-[K_d]”.

Contents of CD can be found at:
[http://s3-eu-west-1.amazonaws.com/
ab22g08/comp3020.zip](http://s3-eu-west-1.amazonaws.com/ab22g08/comp3020.zip)

Bibliography

- [1] AVR C Runtime Library, 2005,
<http://www.nongnu.org/avr-libc/>.
- [2] QT User Interface Library, 2010,
<http://qt.nokia.com/products/>.
- [3] Boost C++ Libraries, 2011,
<http://www.boost.org/>.
- [4] Chris Anderson. Ardupilot Project,
<http://diydrones.com/profiles/blogs/ardupilot-main-page>.
- [5] Ardupilot. ArduPilot Mega Binary Communication Protocol,
<http://code.google.com/p/ardupilot-mega/wiki/Protocol>.
- [6] Atmel. *Application Note; AVR221: Discrete PID controller*, 2006.
- [7] Atmel. *Application Note; AVR042: AVR Hardware Design Considerations*, 2010.
- [8] Atmel. *ATmega168PA Datasheet*, 2010.
- [9] Atmel. *ATmega8 Datasheet*, 2010.
- [10] Eugene Blanchard. H-bridge using P and N channel FETs, 2007,
<http://www.armory.com/~rstevew/Public/Motors/H-Bridges/Blanchard/figure-1.htm>.
- [11] Draganfly Innovations Inc. How Coaxial RC Helicopters Work, 2008,
<http://bit.ly/fADUp7>.
- [12] E-Sky. E-Sky Lama V4, 2010,
http://en.esky-sz.cn/products_index.html.

- [13] Terraneo Federico. QAsyncSerial Class, 2009,
http://www.webalice.it/fede.tft/serial_port/serial_port.html.
- [14] Peter Fleury. I2C Master Interface Library, 2005,
http://homepage.hispeed.ch/peterfleury/group__pfleury__ic2master.html.
- [15] Christopher Garber. Etching a Printed Circuit Board with the Toner Transfer Method, 2005,
http://gilmore2.chem.northwestern.edu/projects/garbz2_prj.php.
- [16] Robert K. Heffley. *A Compilation and Analysis of Helicopter Handling Qualities Data; Volume II: Data Analysis*. 1979.
- [17] Honeywell. *HMC5843 Datasheet*, 2009.
- [18] Nathaniel Lewis. Libjoystick++, 2009,
<http://libjoystick.sourceforge.net/>.
- [19] Maplin. 3 Channel Helicopter with Gyroscope Stabilizer, 2010,
<http://www.maplin.co.uk/3-channel-helicopter-with-gyroscope-stabilizer-35145>
- [20] Maxbotix. Ultrasonic Distance Sensors, 2011,
<http://www.maxbotix.com/>.
- [21] Bernard Mettler, Mark B. Tischler, and Takeo Kanade. System Identification of Small-Size Unmanned Helicopter Dynamics. *American Helicopter Society 55th Forum*, 1999.
- [22] Microchip. *PIC16G87X Datasheet*, 2001.
- [23] Microchip. *Application Note; AN996: Designing a Digital Compass Using the PIC18F2520*, 2010.
- [24] Lito Montala. Chapter 2 : Why and How Helicopters Fly, 2005,
http://www.rcaeronautics4dodos.filipinovegetarianrecipe.com/how_helicopters_fly.htm.
- [25] NXP. *UM10204: I²C-bus specification and user manual*, 2007.
- [26] William Premierlani and Paul Bizard. Direction Cosine Matrix IMU: Theory,
<http://code.google.com/p/gentlenav/>. 2009.
- [27] Lattice Semiconductor. *Technical Note; TN1068: Power Decoupling and Bypass Filtering for Programmable Devices*, 2004.

-
- [28] Sparkfun. 9 Degrees of Freedom Sensor Stick, 2011,
<http://www.sparkfun.com/products/10321>.
 - [29] Laipac Tech. *TLP434 & RLP434 Datasheet*, 2010.
 - [30] Texas Instruments: Laszlo Balogh. *SLUP169: Design and Application Guide for High-Speed MOSFET Gate Drive Circuits*, 2006.
 - [31] Alexander Thomas. Creating PCBs with the toner transfer method, 2006,
<http://www.dr-lex.be/hardware/tonertransfer.html>.
 - [32] Lionel Warnes. *Analogue and Digital Electronics*. Macmillan Press Ltd, 1998.
 - [33] XAircraft. XAircraft X650, 2010,
<http://www.xaircraft.com/wiki/Home/en>.